Chemistry & Biology, Vol. 11, 1239–1250, September, 2004, ©2004 Elsevier Ltd. All rights reserved. DOI 10.1016/j.chembiol.2004.06.009

The Binding Selectivity of ADAR2's dsRBMs Contributes to RNA-Editing Selectivity

Olen M. Stephens, Brittany L. Haudenschild, and Peter A. Beal*
Department of Chemistry
University of Utah
Salt Lake City, Utah 84112

Summary

ADAR2 is an RNA editing enzyme that deaminates adenosines in certain duplex structures. Here, we describe the role of its RNA binding domain, consisting of two copies of a common dsRNA binding motif (dsRBM), in editing site selecivity. ADAR2's dsRBMs bind selectively on a duplex RNA that mimics the Q/R editing site in the glutamate receptor B-subunit pre-mRNA. This selectivity is different from that of PKR's dsRBM I, indicating that dsRBMs from different proteins possess intrinsic binding selectivity. Using directed hydroxyl radical cleavage data, molecular models were developed that predict important recognition surfaces on the RNA for identified dsRBM binding sites. Blocking these surfaces by benzyl modification of guanosine 2-amino groups impeded RNA-editing, demonstrating a correlation between deamination efficiency by ADAR2 and selective binding by its dsRBMs. In addition, the editing activity of a mutant of ADAR2 lacking dsRBM I on N^2-benzylguanosine-modified RNA suggests the location of the dsRBM I binding site that leads to editing at the GluR-B Q/R site.

Introduction

Duplex RNA has drawn increasing attention due to its role in a variety of biological processes including the interferon antiviral response [1], RNA interference [2], and RNA editing [3]. However, the structural elements that lead to specific cellular recognition of duplex RNA structures remain mysterious. These issues are becoming increasingly important to a broad community as the use of duplex RNAs becomes commonplace in gene silencing experiments via RNA interference. Members of a family of proteins with common sequence motifs, dsRBMs (*d*ouble-stranded *R*NA-*b*inding *m*otifs), share the ability to bind duplex RNA in order to carry out functions as diverse as ribonuclease activity (Dicer) [4], mRNA transport (Staufen) [5], RNA editing (ADARs) [6], and protein phosphorylation (PKR) [7]. Members of this family possess varying catalytic activity and RNA binding selectivity. Due to the high degree of sequence similarity in their RNA binding domains, binding selectivity of these proteins has often been ascribed to structures outside the dsRBMs. Furthermore, the lack of a strict sequence requirement for the binding of dsRBM proteins has led to the widespread belief that these motifs only confer general duplex RNA binding affinity with little sequence preference. In this work, we explore the role of the dsRBMs in substrate recognition by the RNA-editing enzyme ADAR2 and compare the observed binding selectivity to that of the RNA-dependent protein kinase, PKR.

ADARs (adenosine deaminases that act on dsRNA) are duplex RNA binding proteins that catalyze the deamination of adenosine (A) to give inosine (I) at specific positions in pre-mRNA transcripts [8]. Since inosine is translated as guanosine, the structural change is functionally a guanosine for adenosine replacement in the mRNA. A number of mRNAs are known to arise from RNA editing through adenosine deamination in a variety of organisms from *Caenorhabditis elegans* to humans [9–12]. An important consequence of this reaction is that the sequences of certain proteins present at a given time in an organism are different from those predicted by the gene sequences. In several examples, properties of the products of translation from edited and unedited RNAs have been studied, indicating that the proper function of the gene product requires efficient editing of its mRNA [10, 13–16]. Interestingly, several of the translation products of messages known to be edited by ADARs are neuronal ligand-gated and voltage-gated ion channels. Thus, RNA-editing by adenosine deamination is a mechanism used to diversify protein function in the nervous system. In one specific example, ADARs deaminate genomically encoded adenosines in the mRNA for the glutamate-gated ion channel B-subunit (GluR-B). In this large RNA, there are only a few editing sites and only two that lead to codon changes. At one of these sites, a glutamine codon (CAG) is converted to a sequence translated as arginine (CIG) (the Q/R site) [9]. The resulting structural change in the channel alters its ion conductance [13, 15].

The majority of research in RNA editing carried out to this point has focused on the identification of the enzymes and substrates involved and the consequence of the editing reaction on the function of the gene products. However, an understanding of the RNA-editing mechanism is lagging. Thus, basic questions, such as why a certain nucleotide in an mRNA molecule is susceptible to editing while others are not, often cannot be effectively answered at this time. Beyond the requirement for the edited adenosine to be in duplex secondary structure, it is not clear to what extent dsRBMs control editing selectivity for ADARs. Do the dsRBMs simply impart a general affinity for dsRNA or are certain binding sites along a dsRNA occupied selectively? If binding selectivity is observed for an ADAR's dsRBMs, do the locations of these binding sites correlate with the location of adenosines that are efficiently edited?

Herein we demonstrate that the dsRBMs of ADAR2's RNA binding domain bind selectively to locations adjacent to the GluR-B Q/R editing site on a model RNA duplex containing this site. The observed binding selectivity is different from that of a dsRBM found in the RNA-dependent protein kinase (PKR), supporting the

*Correspondence: beal@chemistry.utah.edu

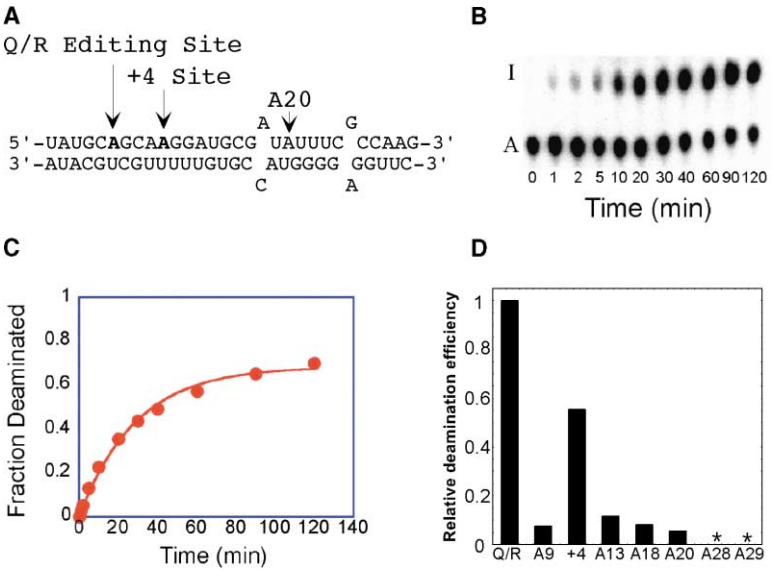

Figure 1. Development of a Q/R Editing Site Substrate

(A) Duplex RNA structure of the Q/R substrate used in this study. Q/R site refers to the position analogous to the adenosine located at the glutamine to arginine editing site found in the GluR-B subunit pre-mRNA [9].

(B) Storage phosphor autoradiogram of TLC plate used to separate deamination products arising from reaction of 150 nM ADAR2 with 25 nM native Q/R substrate.

(C) Plot of product formation as a function of time for the single turnover reaction of ADAR2 and the native Q/R substrate.

(D) Editing selectivity on the model Q/R substrate assessed by cleavage of product RNA at guanosine and inosine sites with E46Q RNase T1. The E46Q mutation in RNase T1 enhances reactivity at inosine positions [42]. ADAR2-dependent increase in cleavage efficiency by E46Q RNase T1 is plotted relative to the most efficiently cleaved nucleotide (Q/R site) as the average from two independent experiments. "*" denotes no detectable increase in cleavage by E46Q RNase T1.

hypothesis that dsRBMs from different proteins possess intrinsic binding selectivity that influences substrate specificity for the parent protein. Using directed hydroxyl radical cleavage data, molecular models were developed that predict important contact surfaces for binding into preferred sites found on this duplex for ADAR2's dsRBMs. Blocking these surfaces with site-specific benzyl modification at guanosine 2-amino groups impeded RNA-editing, demonstrating a correlation between the deamination efficiency of ADAR2 and selective binding by its dsRBMs. Furthermore, the editing activity of a mutant of ADAR2 lacking dsRBM I on N^2-benzylguanosine-modified RNA suggests the location of the dsRBM I binding site that leads to editing at the Q/R site.

Results

Generation of a GluR-B Q/R Minimal Substrate

Using predicted secondary structures of the GluR-B Q/R editing site, a 30 bp duplex substrate was developed for these studies. The sequence originates from the human GluR-B pre-mRNA surrounding the Q/R site, with a complementary strand derived from a downstream intronic sequence, predicted to base pair proximal to the editing site (Figure 1A) [9]. This substrate places the Q/R editing site five base pairs from the 5′ end of the edited strand. This minimal substrate was edited by ADAR2 at the Q/R site in vitro at approximately 70% efficiency (Figures 1B and 1C). Editing is not as efficient as seen at the Q/R site in vivo (100%) and this could be due to the instability of the duplex structure isolated from the remainder of the GluR-B pre-mRNA [9]. However, an adenosine four nucleotides 3′ to the Q/R site in this duplex (the +4 site) is also deaminated by ADAR2 to approximately 50% of the level seen at the Q/R site (Figure 1D). This result is similar to that observed on the GluR-B pre-mRNA in vivo, where the +4 site is edited to ~40% that seen at the Q/R site [9]. No other ADAR2-induced deamination sites are observed on this model Q/R site duplex. Thus, the ADAR2 editing site selectivity observed on the model Q/R duplex studied here mirrors that seen for the full-length GluR-B pre-mRNA in vivo.

ADAR2 dsRBM I Binding on the Q/R Minimal Substrate

We used directed hydroxyl radical cleavage with EDTA•Fe modified proteins to determine if the dsRBMs of ADAR2'sRNA binding domain bound at specific sites on the Q/R site duplex described above [17]. Amino acid positions were chosen for incorporation of EDTA•Fe into ADAR2's dsRBMs using sequence alignments to PKR's dsRBMs (Figure 2). Similar sites of EDTA•Fe modification in PKR have been used to generate cleavage data with a number of dsRNA ligands of PKR [18, 19]. Furthermore, four high-resolution structures of dsRBMs have been published, displaying the same α–β–β–β–α fold, which we assume ADAR2's dsRBMs possess [20–24]. Based on the Xlrbpa dsRBM II-RNA crystal structure [23] and NMR structure of Staufen's dsRBM III bound to an RNA stem-loop [24], we can identify residues in ADAR2's dsRBMs likely to be near the RNA binding surface. T96 (dsRBM I) and F251 (dsRBM II) are located along strand β1, near the center of the RNA binding surface for their respective dsRBMs (Figure 3A). M84 is located on α1 of dsRBM I, roughly on the opposite side of the predicted binding surface from T96 and near one end (Figure 3A). Cysteines were incorporated at these positions in human ADAR2's RNA binding domain (aa 71–316, comprising both dsRBMs and linker polypeptide [25]) using site-directed mutagenesis (Figure 2). We refer to this protein as R-R for dsRBM I and dsRBM II. Each mutant R-R protein was modified with bromoacetamidobenzyl-EDTA•Fe [26], a cysteine selective reagent, to introduce the hydroxyl radical generator at these sites. Electrospray ionization mass spectrometry confirmed the stoichiometric modification of each protein. Quantitative gel mobility shift experiments were carried out to ascertain the effect each mutation and EDTA•Fe modification has on RNA binding affinity (see

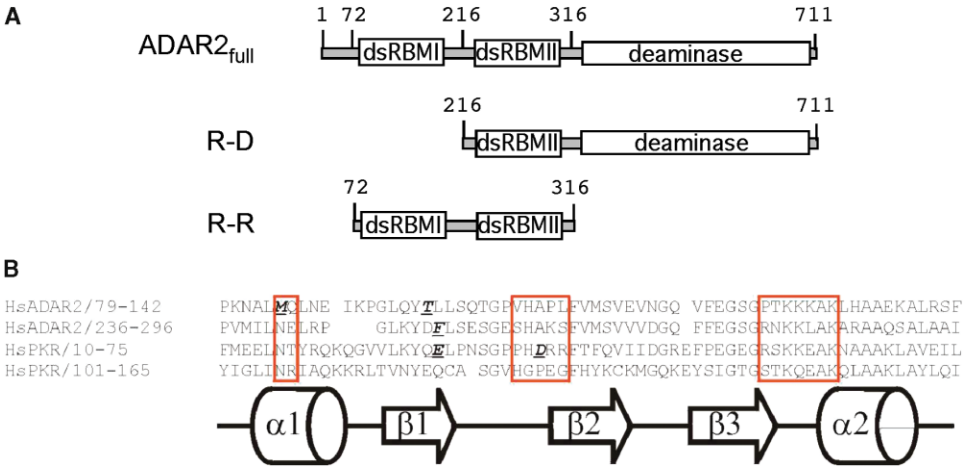

Figure 2. ADAR Proteins Studied and dsRBM Sequence Alignment

(A) Domain maps and select amino acid locations for full-length ADAR2, R-D, and R-R proteins.

(B) Sequence alignments for four dsRBMs, (dsRBM I and dsRBM II from ADAR2 and PKR, respectively.) Residues contained in red boxes are predicted to contact dsRNA ligands based on the Xlrbpa dsRBM II-RNA complex structure [23]. Predicted secondary structural elements are depicted below the corresponding sequences of dsRBMs. Residues mutated to cysteine and modified with bromoacetamidobenzyl-EDTA•Fe for directed hydroxyl radical cleavage experiments are designated in bold.

Supplemental Data available at http://www.chembiol.com/cgi/content/full/11/9/1239/DC1). In each case, the mutation causes less than a 10-fold decrease in affinity (M84C: 1.3-fold; T96C: 9.8-fold; F251C: 6.8-fold), with the modification reaction inducing an approximate 3-fold further affinity decrease.

Directed hydroxyl radical cleavage experiments using M84C-EDTA•Fe and the Q/R site duplex revealed one major cleavage site 3′ to the editing site and approximately in the middle of this minimal substrate (Figure 3B). T96C-EDTA•Fe generates two major cleavage patterns on the Q/R site substrate, straddling the cleavage site observed with M84C-EDTA•Fe (Figure 3C). Several lines of evidence indicate that the cleavage patterns observed are indicative of selective binding by dsRBM I, not the indiscriminant cleavage one might expect if the dsRBM bound the RNA without selectivity. Nor do they arise from unbound EDTA•Fe-modified protein in solution or from hyperreactive nucleotides in the RNA. First, the cleavage is localized to specific nucleotides on the duplex with the sites of efficient cleavage on the two different strands corresponding to base-paired locations (e.g., $C_{16}G_{17}A_{18}$ [top strand] and $C_{14}G_{15}$ [bottom strand] for M84C-EDTA•Fe). The cleavage patterns are only observed for the combination of modified protein and the reagents necessary to generate the hydroxyl radicals from the tethered EDTA•Fe, i.e., hydrogen peroxide and sodium ascorbate. Furthermore, no cleavage is observed with unmodified protein in the presence of free EDTA•Fe in solution and the cleavage reagents (Lane 4 in each Figures 3B–3D). Importantly, the cleavage patterns change when the EDTA•Fe is moved to a new location in the dsRBM in a manner consistent with the relative location of the amino acid positions modified (see below). Also, the cleavage patterns observed for the M84C-EDTA•Fe and T96C-EDTA•Fe proteins are unchanged for a Q/R duplex with the A•C and G•G mismatches converted to A•U and G•C base pairs, respectively (data not shown). Finally, the cleavage pattern observed with an EDTA•Fe-modified dsRBM from PKR's RNA binding domain is distinctly different from that observed with any of the R-R variants from ADAR2 (see below).

The cleavage data from M84C-EDTA•Fe and T96C-EDTA•Fe were used to build models of ADAR2's dsRBM I bound to the Q/R editing site duplex (Figure 3D). The α carbon skeleton from the Xlrbpa dsRBM II structure, highlighting the approximate locations of M84C and T96C, was docked onto a dsRNA helix, modeled with the Q/R substrate sequence, depicting cleavage data collected from M84C-EDTA•Fe and T96C-EDTA•Fe. In these models, nucleotides cleaved by T96C-EDTA•Fe and M84C-EDTA•Fe were aligned closely to the location of the appropriate EDTA•Fe appendage. Significantly, the two modified proteins cleave the RNA duplex on opposite faces of the helix, consistent with the predicted relative locations of M84 and T96 on opposite sides of the RNA binding surface of dsRBM I. To explain these patterns, two dsRBM binding sites are depicted in our models on opposite faces of the helix and orthogonal to the nucleotides cleaved by the modified proteins. The models are consistent with the hypothesis that the single cleavage site generated by M84C-EDTA•Fe is the result of two different complexes, since each of these complexes could direct the EDTA•Fe tethered at the M84C position into similar minor groove locations (Figure 3D). Importantly, the models predict binding surfaces on the RNA that would be critical to complex formation. This information was used in the design of experiments to test the importance of these surfaces in RNA editing by ADAR2 at the Q/R site (see below).

ADAR2 dsRBM II Binding on the Q/R Minimal Substrate

F251C-EDTA•Fe was used to probe ADAR2's dsRBM II binding selectivity on the Q/R editing site substrate. As seen with T96C-EDTA•Fe, two major cleavage sites are revealed 3′ to the editing site (Figure 3E). These sites

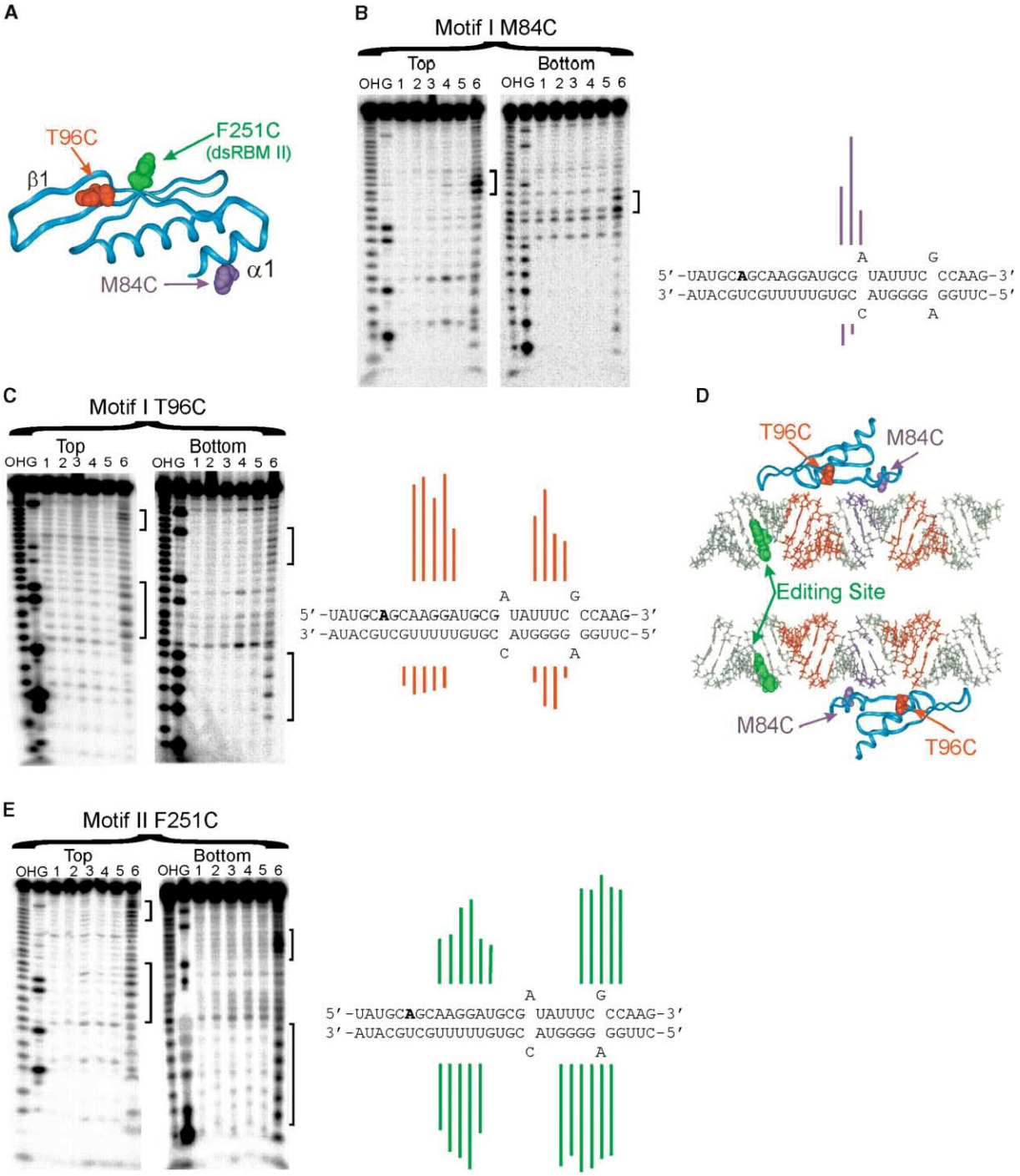

Figure 3. Identification of Binding Sites on Q/R Editing Site Substrate for ADAR2's dsRBMs

(A) The α carbon skeleton of the published Xlrbpa dsRBM II structure was used as a model for the structure of ADAR2's dsRBMs. The three locations for cysteine incorporation are depicted in CPK. T96C and M84C are dsRBM I mutants; F251C is a dsRBM II mutant.

(B) Directed hydroxyl radical cleavage of the Q/R substrate using the EDTA-Fe modified M84C R-R mutant. Shown on the left is a storage phosphor autoradiogram of a 15% denaturing polyacrylamide gel separating the 5′-end labeled RNA cleavage products. Major cleavage sites are identified with brackets. Each gel has the following reaction conditions as labeled: -OH, alkaline hydrolysis; G, T1 RNase; lane 1, RNA with no added hydrogen peroxide or sodium ascorbate; lane 2, RNA in the presence of 4 μM EDTA, 4 μM ferrous ammonium sulfate, 0.001% hydrogen peroxide, and 5 mM sodium ascorbate; lane 3, 4 μM unmodified M84C R-R and RNA with no added hydrogen peroxide or sodium ascorbate; lane 4, 4 μM unmodified M84C R-R and RNA in the presence of 4 μM EDTA, 4 μM ferrous ammonium sulfate, 0.001% hydrogen peroxide, and 5 mM sodium ascorbate; lane 5, 4 μM M84C-EDTA•Fe and RNA with no added hydrogen peroxide or sodium ascorbate; lane 6, 4 μM M84C-EDTA•Fe and RNA in the presence of 0.001% hydrogen peroxide and 5 mM sodium ascorbate. Shown at the right is the mapping of the major cleavage sites on the Q/R substrate secondary structure. Lines indicate sites of cleavage and line lengths indicate relative cleavage efficiencies.

appear to overlap with those of T96C-EDTA•Fe, indicating that dsRBM I and dsRBM II can bind at similar locations on this RNA. The overlap of binding for the two motifs is not necessarily surprising given that these motifs share 53% sequence identity [6]. Interestingly, EDTA•Fe modifications in dsRBM II at positions similar to M84 of dsRBM I (M238C-EDTA•Fe and N241C-EDTA•Fe) did not generate proteins that cleaved RNA. An ~70 amino acid polypeptide links the carboxyl terminus of dsRBM I and amino terminus dsRBM II. Since positions analogous to M84C would be found in the α1 of dsRBM II, located at the amino terminus of this motif, the linker polypeptide could shield the duplex RNA ligand from hydroxyl radical cleavage. Nonetheless, given their similarity, it is likely that the orientation for the two motifs is the same on these binding sites, however, this has not yet been established.

PKR dsRBM I Binding on the Q/R Minimal Substrate

The directed hydroxyl radical cleavage experiments described above establish that ADAR2's dsRBMs can bind a duplex RNA ligand selectively. However, it remained a possibility that the binding selectivity observed was primarily due to the RNA structure and represented a selectivity common to all dsRBMs. Indeed, dsRBM I and dsRBM II of ADAR2 appear to bind in a similar fashion. To compare the intrinsic selectivity of ADAR2's dsRBMs to another member of the dsRBM protein family, PKR's RNA binding domain was used for cleavage experiments on the Q/R editing substrate. The E29C and D38C mutants in dsRBM I of PKR's RNA binding domain were modified with EDTA•Fe as previously described [18]. DsRBM I of PKR shares 31% sequence identity with dsRBM I of ADAR2 (Figure 2). E29C lies along β2 and is roughly in the middle of dsRBM I at a position analogous to T96C (dsRBM I) and F251C (dsRBM II) of ADAR2. D38C is close to one of the ends of the dsRBM positioned in loop 2 between β1 and β2 (Figure 4A). These modified proteins were allowed to react with the Q/R substrate and the cleaved nucleotides were mapped and modeled as with the ADAR2 mutants (Figures 4B and 4C). The cleavage data reveals only one binding site for PKR's dsRBM I on the Q/R substrate. When these results are used to model PKR's dsRBM I on the Q/R substrate, the model reveals a unique binding site, different from either of ADAR2's dsRBMs (Figure 4D). This result confirms that, though dsRBMs are structurally similar, they display different binding selectivities.

The Effect of Introduction of N^2-Benzylguanosine into the Q/R Minimal Substrate

The models generated from the directed hydroxyl radical cleavage experiments predict binding sites for ADAR2's dsRBM I on the Q/R site duplex. In order to determine if these binding sites are important for ADAR2 editing at the Q/R adenosine, we sought to alter the sites by occluding binding surfaces predicted to have contacts to the dsRBM. From high-resolution structures of dsRBM-RNA complexes, it is apparent that crucial contacts are made in minor grooves of the dsRNA ligands [23, 24]. Incorporating bulky, chemically inert substituents at specific minor groove locations allows for the probing of distinct binding sites. This approach has been used successfully to disrupt binding at individual sites on an RNA ligand for PKR by site-selective incorporation of N^2-benzylguanosine [27].

N^2-Benzylguanosine (G^{N2Bn}) was incorporated into the Q/R substrate at the approximate locations predicted to be in contact with the dsRBM using a phosphoramidite recently described [27]. The placement of N^2-benzylguanosine was restricted to purine substitutions on the bottom strand (Figures 5A and 5B). It is more efficient to limit N^2-benzylguanosine placement to the unlabeled strand that can be hybridized to the internally labeled edited strand. Purines were chosen in an attempt to minimize the effect on the overall structure of the substrate. These limitations often preclude optimal placement of the benzyl group in the minor groove. However, the size of the benzyl substituent should still cause detrimental effects on complex formation at or near the modified site.

The Q/R substrate was synthesized in three different benzylated forms as follows: two substrates were designed to inhibit binding at the sites observed ($A6G^{N2Bn}$ and $A12G^{N2Bn}$), while the third benzylated RNA was a control substrate, $G9G^{N2Bn}$, that blocked a surface perpendicular to the predicted binding sites (Figures 5B and 5D). Gel mobility shift experiments were performed to examine the effect of benzylation on the general duplex RNA structure of the benzylated substrates. All of the substrates were completely bound with comparable binding affinities by ADAR2 (Figure 5C). This would suggest that the overall RNA structure is not affected for any of the substrates. However, the gel mobility shift experiments with dsRBM proteins do not provide information concerning binding at specific sites along the RNA. Rather, the benzyl modification likely alters the equilibrium between various protein•RNA complexes, which may be indistinguishable in the gel shift experiment (see below).

The rates of deamination by ADAR2 on these benzylated substrates were compared under single turnover conditions. Both the $A6G^{N2Bn}$ and $A12G^{N2Bn}$ mutations diminished deamination efficiency relative to the native Q/R editing site substrate (Figure 5E, Table 1), indicating that both binding sites are important for deamination. Furthermore, the benzyl group did not affect the rate of

(C) Directed hydroxyl radical cleavage of the Q/R substrate using of T96C-EDTA•Fe. Each lane represents the same reaction conditions as with Figure 3B, using 2 μM of the appropriate T96C variant of R-R.

(D) Models generated in Insight II using the α carbon skeleton from the Xlrbpa dsRBM II structure to model potential binding sites identified by the cleavage experiments. Nucleotides cleaved by M84C-EDTA•Fe are highlighted in purple. Nucleotides cleaved by T96C-EDTA•Fe are highlighted in red. The Q/R editing site is depicted in green CPK.

(E) Directed hydroxyl radical cleavage of the Q/R substrate using F251C-EDTA•Fe. Each lane represents the same reaction conditions as with Figure 3B, using 2 μM of the appropriate F251C variant of R-R.

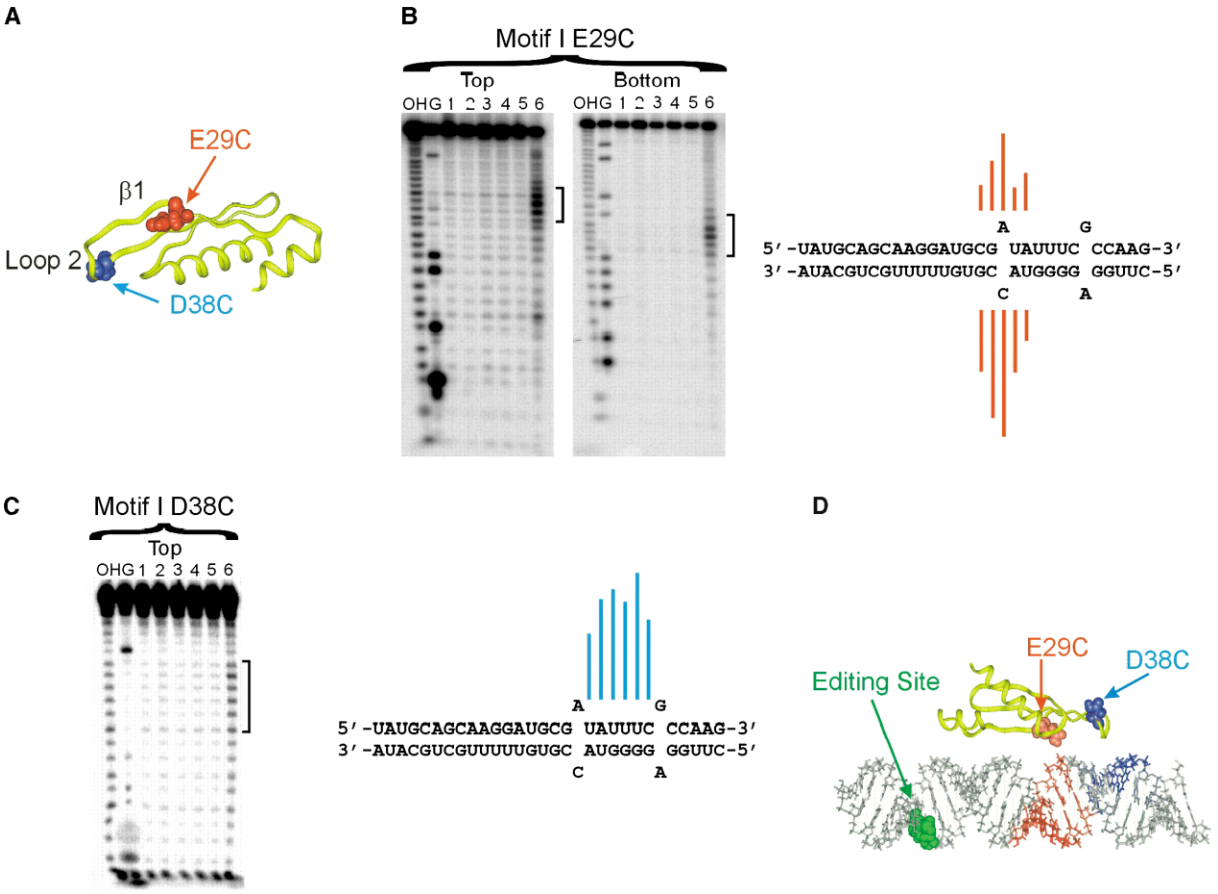

Figure 4. Identification of Binding Surfaces on Q/R Substrate for PKR's dsRBM I

(A) The two locations on the PKR dsRBD were chosen for cysteine incorporation, E29C and D38C in dsRBM I, are depicted in CPK.

(B) Directed hydroxyl radical cleavage of the Q/R substrate using 4 μM E29C-EDTA•Fe. Each lane represents the same reaction conditions as with Figure 3B, using the appropriate E29C variant of PKR's dsRBD.

(C) Directed hydroxyl radical cleavage of the Q/R substrate using 4 μM D38C-EDTA•Fe. Each lane represents the same reaction conditions as with Figure 3B, using the appropriate D38C variant of PKR's dsRBD. The α carbon skeleton from the Xlrbpa dsRBM II structure [23] is used to model the potential binding site identified by the directed hydroxyl radical cleavage experiments. Nucleotides cleaved by E29C-EDTA•Fe are highlighted in red. Nucleotides cleaved by D38C-EDTA•Fe are highlighted in blue.

deamination for the control substrate, emphasizing that the effect is site-specific (Figure 5E, Table 1). The magnitude of the effect from benzylation differed for the two binding sites (A6G^{N2Bn}: k_{rel} = 0.28, A12G^{N2Bn}: k_{rel} = 0.05), suggesting the site inhibited by the A12G^{N2Bn} mutation may be more important. However, this difference could represent inaccuracies in our models or the inability to optimally place the *N*^{2}-benzylguanosine as mentioned above. To test whether this effect was based on the sequence change or introduction of the benzyl group, new substrates were prepared with the simple A to G sequence change, A12G and A6G. The A12G mutation still had a deleterious effect, (A12G: k_{rel} = 0.13), whereas A6G had little effect on deamination (A6G: k_{rel} = 0.72), implying that the benzyl group was primarily responsible for the diminished deamination for the A6G^{N2Bn} mutant (Figure 5E, Table 1). The substantial effect on deamination by a single base change (A12G) suggests that crucial contacts have been disrupted between the RNA and protein at this site.

Since the +4 site adenosine on the model Q/R duplex is also deaminated by ADAR2, we determined if the A12G mutation had an effect at this site by comparing the deamination efficiencies for the Q/R and +4 sites on native sequence and A12G mutant RNA substrates (Figure 5F). While deamination efficiency at the Q/R site is substantially decreased by the A12G mutation, minimal effect is realized for reaction at the +4 site. Thus, this dsRBM binding site is important for deamination by ADAR2 at the Q/R site and not at the +4 site.

The deamination kinetics for substrates bearing site-specific benzyl modifications in the minor groove indicated both the binding sites on the Q/R duplex are important for editing by ADAR2 at the Q/R adenosine. The cleavage patterns for the T96C-EDTA•Fe and F251C-EDTA•Fe proteins are similar and indicate that both dsRBM I and dsRBM II have the potential to bind at either site. Thus, it was not apparent from these results alone which motif occupies which site during the deamination reaction at the Q/R site. To address this issue, we analyzed the effect these modifications had on deamination by a deletion mutant of ADAR2 lacking dsRBM I

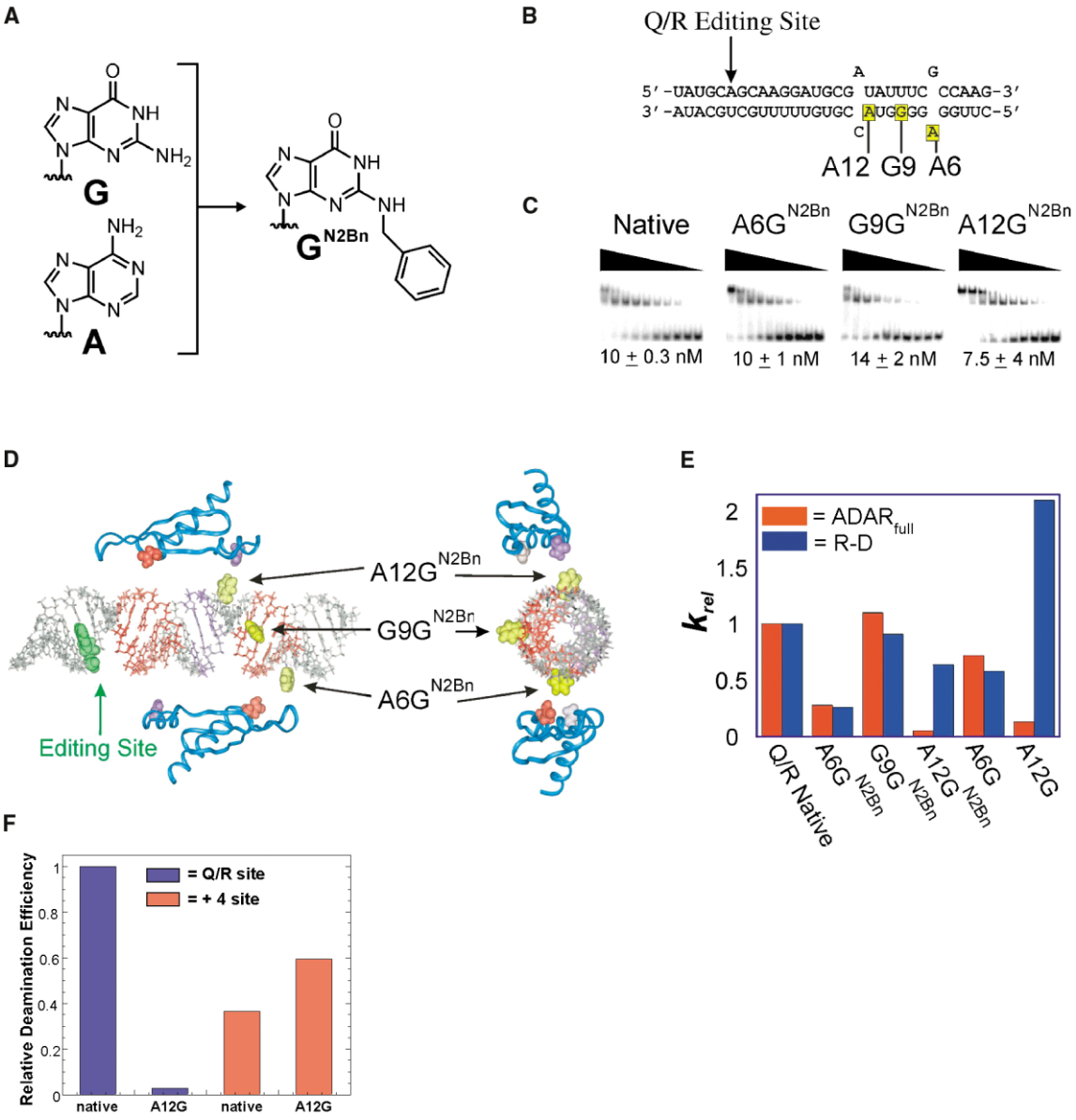

Figure 5. Effect of Mutation of ADAR2 dsRBM Binding Sites on Q/R Editing Site Substrate

(A) N^2-Benzylguanosine (G^{N2Bn}) introduces a benzyl group into the minor groove of RNA duplexes.

(B) Three separate Q/R substrates were synthesized with G^{N2Bn} in the bottom strand at positions A6, G9, and A12.

(C) Gel mobility shift experiments were performed on the native Q/R substrate and all three G^{N2Bn} containing Q/R substrates with varying concentrations of ADAR2: 266, 128, 64, 32, 16, 8, 4, 2, 1, and 0 nM ADAR2.

(D) The relative location of the benzyl modifications to the two binding sites for ADAR2's dsRBMs are depicted in yellow.

(E) A bar graph describing the relative rate constants for deamination assays on the GluR-B Q/R editing site substrate analogs from Table 1. All rates are normalized to that of the native Q/R substrate.

(F) Editing efficiency at Q/R site or +4 site on the model Q/R substrate with native sequence or bearing the A12G mutation assessed by cleavage of product RNA at guanosine and inosine sites with E46Q RNase T1. ADAR2-dependent increase in cleavage efficiency by E46Q RNase T1 is plotted relative to the most efficiently cleaved nucleotide (Q/R site) as the average of two independent experiments.

(Figure 2). This protein (human $ADAR2a_{216\text{-}711}$; R-D for dsRBM II + Deaminase domain) has been shown to retain RNA-editing activity on model duplex substrates [28]. Furthermore, since R-D lacks dsRBM I, one would expect it to be insensitive to benzyl modification at a binding site occupied by dsRBM I during catalysis. We measured rates of deamination at the Q/R site on the benzylated substrates by R-D and compared these rates to that measured for the unmodified RNA. The $A6G^{N2Bn}$ mutation diminished deamination efficiency relative to the native Q/R editing site ($A6G^{N2Bn}$: $k_{rel} = 0.26$) (Figure 5E, Table 1). This decrease in rate is nearly identical to that observed for full-length ADAR2. Also, as observed with full-length ADAR2, deamination of the control substrate by R-D was not effected by benzylation ($G9G^{N2Bn}$: $k_{rel} = 0.91$). However, in contrast to the results with full-

Table 1. Deamination Kinetics for Q/R Site Duplex Substrates

	Deamination by ADAR2[a]		Deamination by R-D	
Substrate	Deamination k_{obs} (min^{-1})	k_{rel}[b]	Deamination k_{obs} (min^{-1})	k_{rel}
Q/R Native	$7.6 \times 10^{-3} \pm 2 \times 10^{-3}$	1	$3.3 \times 10^{-3} \pm 0.5 \times 10^{-3}$	1
A6G^{N2Bn}	$2.1 \times 10^{-3} \pm 1 \times 10^{-3}$	0.28	$0.86 \times 10^{-3} \pm 6 \times 10^{-5}$	0.26
G9G^{N2Bn}	$8.4 \times 10^{-3} \pm 2 \times 10^{-3}$	1.1	$3.0 \times 10^{-3} \pm 0.3 \times 10^{-3}$	0.91
A12G^{N2Bn}	$0.35 \times 10^{-3} \pm 0.03 \times 10^{-3}$	0.05	$2.1 \times 10^{-3} \pm 0.2 \times 10^{-3}$	0.64
A6G	$5.5 \times 10^{-3} \pm 1 \times 10^{-3}$	0.72	$1.9 \times 10^{-3} \pm 0.1 \times 10^{-3}$	0.58
A12G	$0.96 \times 10^{-3} \pm 0.3 \times 10^{-3}$	0.13	$6.9 \times 10^{-3} \pm 0.3 \times 10^{-3}$	2.1

[a] Single turnover deamination reactions of Q/R substrates were carried out with 150 nM enzyme and 15 nM RNA substrate in 15 mM TrisHCl (pH 7.1), 3% glycerol, 0.5 mM DTT, 60 mM KCl, 1.5 mM EDTA, 0.003% NP-40, 160 units/mL RNasin, and 1.0 μg/mL yeast tRNA^{Phe}. The data were fit to the equation: $\ln[\text{substrate}] = -k_{obs} \bullet t$.
[b] k_{rel} is equal to the k_{obs} by ADAR2 or R-D determined for each substrate/k_{obs} for the native Q/R substrate by the same protein.

length ADAR2, the A12G^{N2Bn} mutation had little effect on the rate of deamination at the Q/R site by R-D (A12G^{N2Bn}: $k_{rel} = 0.64$). The contrast between full-length ADAR2 and R-D is even more striking when comparing the effect of the simple A12G mutation on the reaction rates. For full-length ADAR2, this mutation caused an 8-fold decrease in single turnover rate of deamination at the Q/R site, whereas the A12G mutation produced a 2-fold *increase* in this rate for R-D (Figure 5E, Table 1). Since R-D lacks dsRBM I, these results suggest the binding site disrupted by mutation at A12 is occupied by dsRBM I.

To further characterize dsRBM binding to modified substrates, we carried out cleavage reactions with the R-R proteins tethered with EDTA•Fe and the various benzylated RNAs. Interestingly, the cleavage reactions are only subtly affected by benzylguanosine substitution in the RNA. However, when T96C-EDTA•Fe is used to cleave the duplex bearing the A12G^{N2Bn}, a small but reproducible difference in the cleavage pattern is observed at the site proximal to the editing site (Figure 6). Cleavage by this protein on the RNA duplex with native sequence generates a cluster of four nearly equally cleaved nucleotides with a maximum centered around nucleotide A10 (+4 site). However, benzylguanosine substitution at position 12 on the complementary strand causes this pattern to split, with two cleavage maxima at A9 and G12 and a minimum at A10. This new pattern is not simply a result of the intrinsic reactivity of these sites in the benzylated duplex since the pattern for the F251C-EDTA•Fe protein is unchanged (data not shown). These results indicate the binding of dsRBM I to this location on the duplex has been altered, which is consistent with the deamination results obtained for full-length ADAR2 and R-D and benzylated RNAs suggesting this is a binding site for dsRBM I. The new cleavage pattern is likely the result of two new closely spaced binding sites for dsRBM I. Also, the change in cleavage pattern indicates the benzyl modification doesn't prevent dsRBM I from binding the duplex, only adjusts its positioning.

Discussion

Members of the ADAR family exhibit exquisite selectivity for the deamination of specific adenosines in pre-mRNA molecules. For instance, in the large GluR-B pre-mRNA, there are only a few editing sites and only two that lead to codon changes [9]. However, to date there is a poor understanding regarding the parameters that control this selectivity. One hypothesis presented states that the catalytic domains of the ADARs control substrate selectivity, and that the dsRBMs require the duplex RNA substrate to consist of a minimal length, independent of sequence. Indeed, Lazinski and coworkers have exchanged RNA binding domains for ADAR1 and ADAR2, two members of the ADAR family that have overlapping but distinct substrate selectivity. These chimeric proteins retain the substrate selectivity of the constitutive deaminase domain [29]. The natural conclusion from their work is that ADAR substrate preference comes from the individual catalytic domains. Additional data

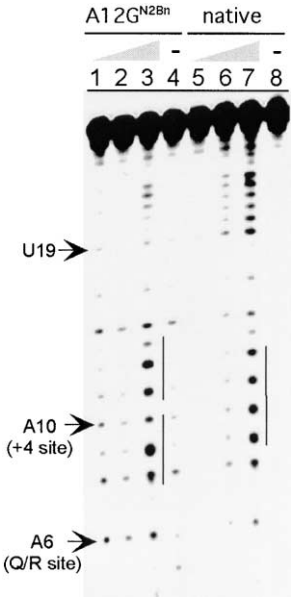

Figure 6. Effect of the A12G^{N2Bn} Modification on Cleavage by T96C-EDTA•Fe

Lanes 1–4, Q/R duplex with A12G^{N2Bn}; lanes 5–8, native Q/R duplex; lanes 1–3 and 5–7, 1, 2, and 4 μM T96C-EDTA•Fe in the presence of 0.001% hydrogen peroxide and 5 mM sodium ascorbate, respectively; lanes 4 and 8, RNA with 6 μM unmodified T96C in the presence of 6 μM EDTA, 6 μM ferrous ammonium sulfate, 0.001% hydrogen peroxide, and 5 mM sodium ascorbate. Indicated are bands corresponding to A6 (Q/R site adenosine), A10 (+4 site adenosine), and U19, which is base paired to the site of benzylation on the complementary strand (G^{N2Bn}12).

has also been collected that implies a limited role for the dsRBM in catalytically active proteins. *Escherichia coli* RNase III possesses an N-terminal dsRBM and a C-terminal endoribonuclease domain. When the protein is expressed lacking its dsRBM, the truncated RNase III retains the ability to efficiently and accurately process dsRNA substrates of the native protein [30]. Furthermore, while the general affinity of the truncated protein is greatly reduced, the catalytic efficiency (k_{cat}/K_m) is essentially unaffected [30]. This implies that the role of the RNA binding domain is simply to provide general binding affinity, lowering the K_m.

In contrast to these studies, a growing body of evidence endorses intrinsic binding selectivity by dsRBMs. A series of chimeric proteins were generated by swapping dsRBMs from ADAR1 and PKR [31]. The results demonstrated that these dsRBMs are not strictly interchangeable and that their binding affects substrate selectivity for deamination and kinase activation [31]. In a similar experiment, dsRBMs of RNase III homologs from *E. coli* and *Rhodobacter capsulatus* were exchanged, and the specificity of the resulting proteins was compared to their native counterparts. The chimeric proteins demonstrated overlapping but distinct selectivity from both native proteins, implying that neither the dsRBM nor the catalytic domains exert dominant control over substrate selectivity [32]. The dsRBM of another RNase III homolog, Rnt1p, displays preferential binding affinity to substrates of the full-length Rnt1p. Changes in the dsRNA substrate that reduced ribonuclease activity had a corresponding deleterious effect on the binding affinity of the dsRBM [33]. Given these conflicting views, we explored the role of the dsRBMs in editing site selectivity for ADAR2.

The strategy we chose to explore the role of ADAR2's dsRBMs in editing site selectivity was to determine if ADAR2's RNA binding domain containing its two dsRBMs displayed any intrinsic binding selectivity on duplex RNA in the absence of the catalytic domain. This was accomplished using EDTA•Fe modification of specific amino acid positions within this protein (R-R). Since EDTA•Fe generates hydroxyl radicals that cleave RNA through oxidative degradation of the ribose, the cleavage reaction itself is largely sequence independent for simple duplex structures [34]. Thus, the cleavage selectivity observed arises from the binding selectivity of the molecule bearing the tethered EDTA•Fe. Since any selective binding identified in this way for the dsRBMs could be influenced by their isolation from the catalytic domain or the modification with EDTA•Fe, we chose to determine the importance of these binding sites in ADAR2 RNA editing by site-specific chemical modification of the binding site followed by analysis of the deamination reaction with the modified RNA.

The results of this study establish that ADAR2's RNA binding domain, comprising both dsRBM I and dsRBM II, does indeed bind selectively on an ADAR2 editing substrate. Additionally, the binding sites identified for ADAR2's dsRBMs are important for efficient editing by the enzyme, since modification at these sites, but not at a control site, decreased the deamination rate. Because the EDTA•Fe proteins used in this study contain both of ADAR2's dsRBMs and the linker sequence between them, it is a formal possibility that the linker is contributing to the selectivity observed. However, we think this unlikely since dsRBM I and dsRBM II bound to similar sites on the RNA tested and the linker would have to contribute equally to selective binding for a motif at both its N and C terminus. Thus, the selectivities observed are more likely to arise from the preferences of the individual dsRBMs in the RNA binding domain. When we compare the binding selectivity of ADAR2's dsRBMs to that of PKR's dsRBMs, we find they possess intrinsically different binding preferences on the same RNA. The implication from this comparative study is that other dsRBMs have the potential for binding preferences that could affect the function of their constitutive proteins. Furthermore, since the dsRBMs from PKR and ADAR2 bind at different sites on the same RNA, the binding selectivity of the two proteins must be dependent on the protein sequence. Thus, both the amino acid sequence of the protein and base composition of the RNA play roles in defining preferred binding sites for dsRBM proteins.

From this work and earlier related studies, we would assert that all dsRBMs could possess intrinsic binding selectivity for specific duplex RNA sequences. In addition to contributing to the understanding of the selectivity observed for dsRBM-containing proteins, this view has implications for investigators using siRNAs for gene silencing experiments. Since there are a number of dsRBM proteins in a cell, competition for binding the ~21 base pair duplex RNAs used in RNA interference experiments might frustrate the gene silencing effort and cause unwanted effects in the cell. For instance, siRNAs that bind well to ADARs may inhibit RNA editing as well as suppress expression of the target gene. In addition, since PKR's dsRBMs demonstrate selective binding for certain RNAs [35], particular siRNAs designed for a specific silencing effect may have the unwanted effect of activating PKR. This effect has been observed for siRNAs designed to inhibit expression of various targets in T98G cells [36].

From deamination kinetic data generated with full-length ADAR2 and the deletion mutant lacking dsRBM I on N^2-benzylguanosine-containing RNA substrates, we are able to suggest the binding sites for each of ADAR2's dsRBMs in the complex leading to Q/R site editing. Q/R site editing by R-D, which lacks dsRBM I, is not significantly inhibited by the A12G^{N2Bn}, whereas the rate of deamination by full-length ADAR2 is decreased by a factor of 20. The A12 position was identified through modeling based on the directed hydroxyl radical cleavage data generated by the R-R mutants bearing the EDTA•Fe in dsRBM I. In addition, the A12G^{N2Bn} modification subtly alters the cleavage pattern by T96C-EDTA•Fe at the site proximal to the Q/R editing site. These data taken together argue that dsRBM I binds at the site altered by the A12G^{N2Bn} modification in the complex leading to Q/R site editing. Since the A6G^{N2Bn} mutation affects Q/R editing by both full-length ADAR2 and R-D, it follows that this mutation disrupts dsRBM II binding. Since the deaminase domain is also common between full-length ADAR2 and R-D, it is possible that the A6G^{N2Bn} mutation affects binding by the deaminase domain. However, we find this explanation unlikely given that (1) this site was

identified through molecular modeling based on directed hydroxyl radical cleavage data generated by EDTA•Fe-modified R-R proteins lacking the deaminase domain and (2) the distance on the RNA between this mutation and the reactive nucleotide, which must bind the deaminase domain during catalysis, is 19 base pairs.

The importance of the RNA sequence distal to the edited adenosine is illustrated by the fact that a single adenosine to guanosine change 13 bp from the Q/R editing site significantly diminishes deamination by ADAR2. The A12G mutation inhibited editing at the Q/R site, which is the major site of deamination on the model substrate, but did not inhibit reaction at the minor site (+4 site), which is consistent with the hypothesis that dsRBM binding at specific locations on the RNA duplex leads to selective editing. The effect of the A12G mutation could be the result of introducing a single 2-amino group in the duplex RNA minor groove or altered hydrogen bonding with the complement base. Interestingly, Emeson and colleagues have recently shown the existence of a cluster of five residues with a bias for specific bases 7–15 nucleotides 3′ to known ADAR2 editing sites [37]. Furthermore, either A or U is present at the position 13 nucleotides 3′ to the site of editing in 19 of the 23 substrates analyzed. Given the data presented here, we would argue this preference arises from selective dsRBM binding at this location on the RNA substrates.

Significance

ADAR enzymes catalyze RNA editing reactions that convert adenosines to inosines in pre-mRNAs encoding a variety of proteins, including receptors for the neurotransmitters glutamate and serotonin. RNA editing of this type appears to be necessary for a properly functioning central nervous system in metazoa. However, an understanding of the basis for the editing selectivity observed for these enzymes is currently lacking. Through a combination of directed hydroxyl radical cleavage experiments, site-specific steric occlusion of RNA minor groove sites, and deamination kinetics, we have established that (1) ADAR2's dsRBMs bind selectively to a duplex RNA structure found in a naturally occurring editing substrate and (2) this binding selectivity contributes to editing efficiency for the native enzyme. Given the demonstrated role for the deaminase domain in editing site selection [29], it is apparent that selective editing by ADAR2 arises from the combination of preferences intrinsic to both the RNA binding domain and the catalytic domain of the enzyme. Deamination kinetics for full-length ADAR2 and a deletion mutant lacking dsRBM I and RNA substrates with specific binding sites altered by steric occlusion in the minor groove have revealed the binding sites for ADAR2's dsRBMs in the complex leading to editing at the Q/R site in GluR-B pre-mRNA. Importantly, the binding selectivity of ADAR2's dsRBMs was shown to be different from that of a dsRBM found in the RNA-dependent protein kinase PKR. Thus, all dsRBMs do not necessarily behave similarly in their RNA binding selectivity. Both the amino acid sequence of the protein and the nucleotide sequence of the RNA are important determinants of preferred sites for dsRBM proteins.

Experimental Procedures

General

Distilled, deionized water was used for all aqueous reactions and dilutions. Biochemical reagents were obtained from Sigma/Aldrich unless otherwise noted. Common enzymes were purchased from Stratagene, Boehringer-Mannheim, or New England Biolabs. E46Q RNase T1 was obtained as a gift from Professor Brenda Bass, Department of Biochemistry, University of Utah. Oligonucleotides were prepared on a Perkin-Elmer/ABI model 392 DNA/RNA synthesizer with β-cyanoethyl phosphoramidites. 5′-Dimethoxytrityl-protected 2′-deoxyadenosine, 2′-deoxyguanosine, 2′-deoxycytidine, and thymidine phosphoramidites were purchased from Perkin-Elmer/ABI. Protected adenosine, guanosine, cytidine, and uridine ribonucleoside phosphoramidites were purchased from Glen Research. [γ-^{32}P]ATP (6000 Ci/mmol) was obtained from DuPont NEN. Storage phosphor autoradiography was carried out using imaging plates obtained from Kodak. A Molecular Dynamics STORM 840 was used to obtain all data from phosphor imaging plates. Liquid scintillation counting was carried out with a Beckman LS 6500 Scintillation Counter and Bio-Safe II cocktail from Research Products International, Corp.

Protein Overexpression, Purification, and EDTA•Fe Modification

Full-length ADAR2 and R-D were overexpressed in *Saccharomyces cerevisiae* and purified as previously described [28, 38]. The human ADAR2 RNA binding domain (amino acids 71–316, R-R) was obtained as a glutathione *S*-transferase (GST) fusion protein by expression in *Escherichia coli* using derivatives of the bacterial expression plasmid pGEX-2T (Amersham Pharmacia Biotech). This fragment contains both dsRBMs and the intervening sequence [25]. The following primers were used to generate the T96C mutant, using the QuikChange mutagenesis kit (Stratagene): 5′-CCTGGTTTGCAGTA C*tgt*CTCCTGTCCCAGACTGGG-3′ and 5′-CCCAGTCTGGGACAGG AG*aca*GTACTGCAAACCAGG-3′. The following primers were used to generate the M84C mutant, using the Quickchange mutagenesis kit (Stratagene): 5′-CCCAAGAACGCCCTG*tgt*CAGCTGAATGAGA CAAG-3′ and 5′-CTTGATCTCATTCAGCTG*aca*CAGGGCGTTCTTT GGG-3′. The following primer was used to create the F251C mutant through a mega primer approach: 5′-CCAGGACTCAAGTATGAC*tgt* CTCTCCGAGAGCGGG-3′. Lowercase letters represent the incorporated mutation. BL-21 *E. coli* (Amersham Pharmacia Biotech) cells were transformed with the mutant plasmid. Overexpression and purification of the protein was carried out as previously described [25]. This protein was modified with bromoacetamidobenzyl-EDTA•Fe as previously described [18]. The modified protein was then analyzed by electrospray mass spectroscopy to confirm modification [18]. The calculated molecular mass for M84C-EDTA•Fe was 26,945 (found, 26,944). The calculated mass for T96C-EDTA•Fe was 26,929 Da (found, 26,936 Da). The calculated molecular mass for F251C-EDTA•Fe was 26,883 Da (found, 26,886 Da). The purity of R-R was estimated to be >95% based on analysis by Coomassie Blue-stained protein gels. The concentration of the modified protein was determined through a Bradford assay using known amounts of bovine serum albumin to generate a standard curve.

Preparation of Q/R Duplex RNAs

The following oligonucleotides were chemically synthesized for the formation of the Q/R dsRNA substrate: 5′-UAUGCAGCAAGGAUGC GAUAUUUCGCCAAG-3′ and 5′-CUUGGAGGGGUACCGUGUUUU UGCUGCAUA-3′. The following chemically synthesized oligonucleotides were used for a chimeric ligation to generate internally labeled substrate: chimeric extension strand 5′-dCdCdTdTdGdGdGdTdGd CdCdTdTrUrArUrGrC-3′, DNA splint 5′-AAATATCGCATCCTTGCTG CATAAAGGCACCCAAGG-3′, and labeled strand 5′-AGCAAGGA UGCGAUAUUUCGCCAAG-3′ [39]. Deprotection of synthetic oligoribonucleotides was carried out in NH_3-saturated methanol for 24 hr at room temperature followed by 0.1 M tetrabutylammonium fluoride in THF for 48 hr at room temperature. Deprotected oligonucleotides

were purified by PAGE, visualized by UV shadowing, and extracted from the gel by the crush and soak method with 0.5 M NH_4OAc, 0.1% SDS, and 0.1 mM EDTA. The oligonucleotides were ethanol-precipitated and redissolved in deionized water. Concentrations were determined by the UV absorbance at 260 nm using extinction coefficients calculated based on the nearest-neighbor approximation [40]. For the formation of Q/R duplex RNAs, the labeled strand was purified by PAGE, and extracted as described above. The purified labeled strand was hybridized to 10 equivalents of unlabeled complement in TE buffer (10 mM Tris-HCl [pH 7.5] and 0.1 mM EDTA) with 200 mM NaCl. The mixture was heated at 95°C in a water bath for 5 min and allowed to slow-cool overnight to room temperature. The duplex was purified on a 10% nondenaturing polyacrylamide gel. The appropriate band was visualized by storage phosphor autoradiography, excised, and extracted into TE buffer overnight at room temperature. Polyacrylamide particles were removed using a Spin-X (Costar) centrifuge column. The RNA duplex was ethanol-precipitated, redissolved in deionized water, and stored at 4°C.

Directed Hydroxyl Radical Cleavage Experiments

RNA complexes with dsRBM-EDTA•Fe conjugates were formed by incubating the protein with 5′-end-labeled RNA at room temperature for 7 min in 25 mM Tris-HCl (pH 7.0), 30 μg/mL $tRNA^{Phe}$, and 10 mM NaCl. Protein-RNA complexes (20 μl final reaction volume) were probed by initiating hydroxyl radical formation with 0.001% hydrogen peroxide and 5 mM sodium ascorbate followed by incubation at room temperature for 10 min. Reactions were quenched with 20 μl of formamide loading dye and analyzed via 15% 19:1 acrylamide:bisacrylamide denaturing polyacrylamide gel electrophoresis. Data were obtained from the gels using storage phosphor autoradiography and a STORM PhosphorImager (Molecular Dynamics). Mapping of the cleavage data was performed using ImageQuant software (Molecular Dynamics). Quantification of cleavage intensity was determined as a percent increase of specific cleavage to a control nucleotide.

Deamination Assay with Internally Labeled Substrate

The activity of ADAR2 on the wild-type Q/R substrate was assayed under single turnover conditions with 150 nM ADAR2 and 25 nM substrate. Single turnover reactions, comparing native and benzylated RNAs were carried out with 150 nM ADAR2, 15 nM labeled RNA duplex, and assay buffer containing 15 mM Tris-HCl (pH 7.1), 3% glycerol, 0.5 mM DTT, 60 mM KCl, 1.5 mM EDTA, 0.003% NP-40, 160 units/mL RNasin, and 1.0 μg/mL yeast $tRNA^{Phe}$. Reaction mixtures were incubated at 30°C for varying times. At each time point, an aliquot was removed and the reaction was quenched by the addition of 0.5% SDS at 95°C, followed by digestion with nuclease P1 and resolution of the resulting 5′-mononucleotides by thin-layer chromatography (TLC) as previously described [41]. Storage phosphor imaging plates (Kodak) were pressed flat against TLC plates and exposed in the dark. The data were analyzed by performing volume integrations of the regions corresponding to starting material, product, and background sites using the ImageQuant software. The data were fit to the equation: $\ln[\text{substrate}] = -k_{obs}t$ where [substrate] is the concentration of adenosine at the editing site, k_{obs} is the deamination rate constant, and t is time.

Deamination Assay Using E46Q RNase T1

The Q/R duplex RNA was 5′-end labeled and purified as described above. The labeled duplex was exposed for 1 hr to the conditions described above for deaminase reactions. A control reaction lacking ADAR2 was also performed. The reactions were stopped by phenol/chloroform extractions and the RNA product was ethanol precipitated. The RNA pellet was resuspended in 20 mM sodium acetate (pH 4.5) containing 1 mg/ml $tRNA^{Phe}$ in a final volume of 10 μL. Samples were heated to 90°C for 2 min and immediately moved to 60°C. After 2 min incubation at 60°C, 0.05 U (as defined by Boehringer Mannheim) E46Q T1 ribonuclease was added. Reactions were allowed to proceed for 15 min at 60°C and were stopped by addition of 10 ml of formamide loading dye and quick freezing in dry ice. The products of these reactions were resolved by PAGE on a 20% 19:1 acrylamide:bisacrylamide gel. Deamination efficiency at individual adenosines was determined as the percent increase in E46Q T1 cleavage from control reaction lacking ADAR2. A background value obtained from a nonreactive nucleotide position was subtracted. These resulting values were normalized to the most efficiently cleaved nucleotide for an RNA strand.

Gel Mobility Shift Assay

Each binding reaction was carried out by combining ADAR2 at varying concentrations with 50 pM 5′-^{32}P end-labeled RNA duplex in 15 mM Tris-HCl (pH 7.9), 3% glycerol, 0.5 mM DTT, 60 mM KCl, 1.5 mM EDTA, 0.003% NP-40, 160 U/mL RNasin, and 1.0 μg/mL yeast $tRNA^{Phe}$ and allowing the mixture to incubate at 30°C for 20 min. Samples were then loaded onto a running 6% nondenaturing polyacrylamide gel (79:1 acrylamide:bisacrylamide) and electrophoresed in 0.5× TBE buffer at 4°C. Storage phosphor imaging plates (Kodak) were pressed flat against the electrophoresis gels and exposed in the dark. The data were analyzed by performing volume integrations of the regions corresponding to free RNA, the ADAR2•RNA complex, and background sites using the ImageQuant software. For the determination of apparent dissociation constants, the data were fit to the equation: fraction bound = [ADAR2]/([ADAR2] + K_d) using the least-squares method of KaleidaGraph.

Synthesis of N^2-benzylguanosine-Containing Oligonucleotides

For the dsRNA substrates containing N^2-benzylguanosine, synthesis of the N^2-benzylguanosine phosphoramidite was carried out as previously described [27]. The modified nucleotide was introduced with a double coupling method on the Perkin-Elmer/ABI model 392 DNA/RNA synthesizer. Deprotection and purification of the modified oligonucleotide followed similar procedures as described above.

Supplemental Data

Supplemental Data for this article can be found at http://www.chembiol.com/cgi/content/full/11/9/1239/DC1.

Acknowledgments

P.A.B. acknowledges financial support from the National Institutes of Health (GM-61115). O.M.S. was supported by a National Institutes of Health training grant (GM-08573).

Received: November 11, 2003
Revised: May 18, 2004
Accepted: June 21, 2004
Published: September 17, 2004

References

1. Stark, G.R., Kerr, I.M., Williams, B.R.G., Silverman, R.H., and Schreiber, R.D. (1998). How cells respond to interferons. Annu. Rev. Biochem. *67*, 227–264.
2. Hannon, G.J. (2002). RNA interference. Nature *418*, 244–251.
3. Bass, B.L. (2002). RNA editing by adenosine deaminases that act on RNA. Annu. Rev. Biochem. *71*, 817–846.
4. Bernstein, E., Caudy, A.A., Hammond, S.M., and Hannon, G.J. (2001). Role for a bidentate ribonuclease in the initiation step of RNA interference. Nature *409*, 363–366.
5. St. Johnston, D., Beuchle, D., and Nusslein-Volhard, C. (1991). Staufen, a gene required to localize maternal RNAs in the *Drosophila* egg. Cell *66*, 51–63.
6. Melcher, T., Maas, S., Herb, A., Sprengel, R., Seeburg, P.H., and Higuchi, M. (1996). A mammalian RNA editing enzyme. Nature *379*, 460–464.
7. Meurs, E., Chong, K., Galabru, J., Thomas, N.S., Kerr, I.M., Williams, B.R.G., and Hovanessian, A.G. (1990). Molecular cloning and characterization of the human double-stranded RNA-activated protein kinase induced by interferon. Cell *62*, 379–390.
8. Bass, B.L., Nishikura, K., Keller, W., Seeburg, P.H., Emeson, R.B., O'Connell, M.A., Samuel, C.E., and Herbert, A. (1997). A standardized nomenclature for adenosine deaminases that act on RNA. RNA *3*, 947–949.
9. Higuchi, M., Single, F.N., Kohler, M., Sommer, B., Sprengel, R.,

and Seeburg, P.H. (1993). RNA editing of AMPA receptor subunit GluR-B: A base-paired intron-exon structure determines position and efficiency. Cell *75*, 1361–1370.

10. Lomeli, H., Mosbacher, J., Melcher, T., Hoger, T., Geiger, J.R.P., Kuner, T., Monyer, H., Higuchi, M., Bach, A., and Seeburg, P.H. (1994). Control of kinetic properties of AMPA receptor channels by nuclear RNA editing. Science *266*, 1709–1713.
11. Polson, A.G., Bass, B.L., and Casey, J.L. (1996). RNA editing of hepatitis delta virus antigenome by dsRNA-adenosine deaminase. Nature *380*, 454–456.
12. Tonkin, L.A., Saccomanno, L., Morse, D.P., Brodigan, T., Krause, M., and Bass, B.L. (2002). RNA editing by ADARs is important for normal behavior in *Caenorhabditis elegans*. EMBO J. *21*, 6025–6035.
13. Hume, R.I., Dingledine, R., and Heinemann, S.F. (1991). Identification of a site in glutamate receptor subunits that controls calcium permeability. Science *253*, 1028–1031.
14. Verdoorn, T.A., Burnashev, N., Monyer, H., Seeburg, P.H., and Sakmann, B. (1991). Structural determinants of ion flow through recombinant glutamate receptor channels. Science *252*, 1715–1718.
15. Burnashev, N., Monyer, H., Seeburg, P.H., and Sakmann, B. (1992). Divalent ion permeability of AMPA receptor channels is dominated by the edited form of a single subunit. Neuron *8*, 189–198.
16. Burns, C.M., Chu, H., Rueter, S.M., Hutchinson, L.K., Canton, H., Sanders-Bush, E., and Emeson, R.B. (1997). Regulation of serotonin-2C receptor G-protein coupling by RNA editing. Nature *387*, 303–308.
17. Schultz, P.G., Taylor, J.S., and Dervan, P.B. (1982). Design and synthesis of a sequence-specific DNA cleaving molecule. J. Am. Chem. Soc. *104*, 6861–6863.
18. Spanggord, R.J., and Beal, P.A. (2001). Selective binding by the RNA binding domain of PKR revealed by affinity cleavage. Biochemistry *40*, 4272–4280.
19. Spanggord, R.J., Vuyisich, M., and Beal, P.A. (2002). Identification of binding sites for both dsRBMs of PKR on kinase-activating and kinase-inhibiting RNA ligands. Biochemistry *41*, 4511–4520.
20. Bycroft, M., Grunert, S., Murzin, A.G., Proctor, M., and St. Johnston, D. (1995). NMR solution structure of a dsRNA binding domain from *Drosophila* staufen protein reveals homology to the N-terminal domain of ribosomal protein S5. EMBO J. *14*, 3563–3571.
21. Kharrat, A., Macias, M.J., Gibson, T.J., Nilges, M., and Pastore, A. (1995). Structure of the dsRNA binding domain of *E. coli* RNase III. EMBO J. *14*, 3572–3584.
22. Nanduri, S., Carpick, B.W., Yang, Y., Williams, B.R.G., and Qin, J. (1998). Structure of the double-stranded RNA-binding domain of the protein kinase PKR reveals the molecular basis of its dsRNA-mediated activation. EMBO J. *17*, 5458–5465.
23. Ryter, J.M., and Schultz, S.C. (1998). Molecular basis of double-stranded RNA-protein interactions: structure of a dsRNA-binding domain complexed with dsRNA. EMBO J. *17*, 7505–7513.
24. Ramos, A., Grunert, S., Adams, J., Micklem, D.R., Proctor, M.R., Freund, S., Bycroft, M., St. Johnston, D., and Varani, G. (2000). RNA recognition by a Staufen double-stranded RNA-binding domain. EMBO J. *19*, 997–1009.
25. Yi-Brunozzi, H.-Y., Stephens, O.M., and Beal, P.A. (2001). Conformational changes that occur during an RNA-editing adenosine deamination reaction. J. Biol. Chem. *276*, 37827–37833.
26. DeRiemer, L.H., Meares, C.F., Goodwin, D.A., and Diamanti, C.J. (1981). BLEDTA II: synthesis of a new tumor-visualizing derivative of cobalt(III)-bleomycin. J. Labelled Compd. Radiopharm. *18*, 1517–1534.
27. Puthenveetil, S., Veliz, E.A., and Beal, P.A. (2004). Site-specific modification of Epstein-Barr virus-encoded RNA 1 with N2-benzylguanosine limits the binding sites occupied by PKR. Chembiochem *5*, 383–386.
28. Macbeth, M.R., Lingam, A.T., and Bass, B.L. (2004). Evidence for auto-inhibition by the N-terminus of hADAR2 and activation by dsRNA binding. RNA, in press.
29. Wong, S.K., Sato, S., and Lazinski, D.W. (2001). Substrate recognition by ADAR1 and ADAR2. RNA *7*, 846–858.
30. Sun, W., Jum, E., and Nicholson, A.W. (2001). Intrinsic double-stranded-RNA processing activity of *Escherichia coli* Ribonuclease III lacking the dsRNA-binding domain. Biochemistry *40*, 14976–14984.
31. Liu, Y., Lei, M., and Samuel, C.E. (2000). Chimeric double-stranded RNA-specific adenosine deaminase ADAR1 proteins reveal functional selectivity of double-stranded RNA-binding domains from ADAR1 and protein kinase PKR. Proc. Natl. Acad. Sci. USA *97*, 12541–12546.
32. Conrad, C., Evguenieva-Hackenberg, E., and Klug, G. (2001). Both N-terminal catalytic and C-terminal RNA binding domain contribute to substrate specificity and cleavage site selection of RNase III. FEBS Lett. *509*, 53–58.
33. Nagel, R., and Ares, M.J. (2000). Substrate recognition by a eukaryotic RNase III: the double-stranded RNA-binding domain of Rnt1p selectively binds RNA containing a 5′-AGNN-3′ tetraloop. RNA *6*, 1142–1156.
34. Pogozelski, W.K., and Tullius, T.D. (1998). Oxidative strand scission of nucleic acids: routes initiated by hydrogen abstraction from the sugar moiety. Chem. Rev. *98*, 1089–1107.
35. Circle, D.A., Neel, O.D., Robertson, H.D., Clarke, P.A., and Mathews, M.B. (1997). Surprising specificity of PKR binding to delta agent genomic RNA. RNA *3*, 438–448.
36. Sledz, C.A., Holko, M., de Veer, M.J., Silverman, R.H., and Williams, B.R.G. (2003). Activation of the interferon system by short-interfering RNAs. Nat. Cell Biol. *5*, 834–839.
37. Dawson, T.R., Sansam, C.L., and Emeson, R.B. (2004). Structure and sequence determinants required for the RNA editing of ADAR2 substrates. J. Biol. Chem. *279*, 4941–4951.
38. Ley, H.L., III. (2001). PhD thesis. Biochemistry Department, University of Utah, Salt Lake City, Utah.
39. Stephens, O.M., Yi-Brunozzi, H.-Y., and Beal, P.A. (2000). Analysis of the RNA-editing reaction of ADAR2 with structural and fluorescent analogues of the GluR-B R/G editing site. Biochemistry *39*, 12243–12251.
40. Cantor, C.R., and Tinoco, I. (1965). Absorption and optical rotatory dispersion of seven trinucleoside diphosphates. J. Mol. Biol. *13*, 65–77.
41. Bass, B.L., and Weintraub, H. (1988). An unwinding activity that covalently modifies its double-stranded RNA substrate. Cell *55*, 1089–1098.
42. Steyaert, J., Opsomer, C., Wyns, L., and Stanssens, P. (1991). Quantitative analysis of the contribution of Glu46 and Asn98 to the guanosine specificity of ribonuclease T1. Biochemistry *30*, 494–499.